



**HAL**  
open science

## **G6PC mRNA Therapy Positively Regulates Fasting Blood Glucose and Decreases Liver Abnormalities in a Mouse Model of Glycogen Storage Disease 1a**

Daniel Roseman, Tayeba Khan, Fabienne Rajas, Lucy Jun, Kirtika Asrani, Cleo Isaacs, Jeremiah Farelli, Romesh Subramanian

► **To cite this version:**

Daniel Roseman, Tayeba Khan, Fabienne Rajas, Lucy Jun, Kirtika Asrani, et al.. G6PC mRNA Therapy Positively Regulates Fasting Blood Glucose and Decreases Liver Abnormalities in a Mouse Model of Glycogen Storage Disease 1a. *Molecular Therapy*, 2018, 26 (3), pp.814-821. 10.1016/j.ymthe.2018.01.006 . inserm-02379178

**HAL Id: inserm-02379178**

**<https://inserm.hal.science/inserm-02379178v1>**

Submitted on 25 Nov 2019

**HAL** is a multi-disciplinary open access archive for the deposit and dissemination of scientific research documents, whether they are published or not. The documents may come from teaching and research institutions in France or abroad, or from public or private research centers.

L'archive ouverte pluridisciplinaire **HAL**, est destinée au dépôt et à la diffusion de documents scientifiques de niveau recherche, publiés ou non, émanant des établissements d'enseignement et de recherche français ou étrangers, des laboratoires publics ou privés.

# G6PC mRNA Therapy Positively Regulates Fasting Blood Glucose and Decreases Liver Abnormalities in a Mouse Model of Glycogen Storage Disease 1a

Daniel S. Roseman,<sup>1</sup> Tayeba Khan,<sup>2</sup> Fabienne Rajas,<sup>3</sup> Lucy S. Jun,<sup>4</sup> Kirtika H. Asrani,<sup>1</sup> Cleo Isaacs,<sup>1</sup> Jeremiah D. Farelli,<sup>1</sup> and Romesh R. Subramanian<sup>1</sup>

<sup>1</sup>Discovery Research, Alexion Pharmaceuticals, Inc., 75 Sidney Street, Cambridge, MA 02139, USA; <sup>2</sup>In Vivo Pharmacology, Alexion Pharmaceuticals, Inc., 33 Hayden Avenue, Lexington, MA 02421, USA; <sup>3</sup>INSERM U1213, Université Claude Bernard Lyon, 69100 Villeurbanne, France; <sup>4</sup>Biomarkers, Alexion Pharmaceuticals, Inc., 100 College Street, New Haven, CT 06510, USA

**Glycogen storage disease type 1a (GSD1a) is an inherited metabolic disorder caused by the deficiency of glucose-6-phosphatase (G6Pase). GSD1a is associated with life-threatening hypoglycemia and long-term liver and renal complications. We examined the efficacy of mRNA-encoding human G6Pase in a liver-specific G6Pase<sup>-/-</sup> mouse model (*L-G6PC<sup>-/-</sup>*) that exhibits the same hepatic biomarkers associated with GSD1a patients, such as fasting hypoglycemia, and elevated levels of hepatic glucose-6-phosphate (G6P), glycogen, and triglycerides. We show that a single systemic injection of wild-type or native human G6PC mRNA results in significant improvements in fasting blood glucose levels for up to 7 days post-dose. These changes were associated with significant reductions in liver mass, hepatic G6P, glycogen, and triglycerides. In addition, an engineered protein variant of human G6Pase, designed for increased duration of expression, showed superior efficacy to the wild-type sequence by maintaining improved fasting blood glucose levels and reductions in liver mass for up to 12 days post-dose. Our results demonstrate for the first time the effectiveness of mRNA therapy as a potential treatment in reversing the hepatic abnormalities associated with GSD1a.**

## INTRODUCTION

Glycogen storage disease type 1a (GSD1a) is an inherited metabolic disorder caused by a deficiency of glucose-6-phosphatase (G6Pase or G6PC), the key enzyme in glucose homeostasis.<sup>1-3</sup> G6Pase catalyzes the terminal reaction of glycogenolysis and gluconeogenesis in liver and kidney and the hydrolysis of glucose-6-phosphate (G6P) to glucose and inorganic phosphate.<sup>4,5</sup>

Failure to produce glucose and the accumulation of intracellular G6P leads to the characteristic pathologies: severe, fasting hypoglycemia; lactic acidemia; hypertriglyceridemia; hyperuricemia; hypercholesterolemia; hepatomegaly; and steatosis.<sup>2,6-8</sup> Therapy is based on strict dietary compliance, which enables patients to maintain normoglycemia and live into adulthood, but underlying pathological processes

continue, resulting in the development of long-term complications.<sup>3,9,10</sup> Of significant concern are the hepatocellular adenomas (HCAs) that develop in 70%–80% of GSD1a patients by their third decade of life.<sup>11-13</sup> HCA transformation into hepatocellular carcinomas (HCCs) occurs in 10% of these patients.<sup>12</sup>

Liver-directed gene therapy has proved successful in correcting the metabolic abnormalities associated with G6Pase deficiency in several GSD1a animal models.<sup>8,10,14-19</sup> However, inherent risks remain in the clinical setting from insertional mutagenesis, immunogenic responses, and carcinogenic effects.<sup>20,21</sup> The development of mRNA-based therapy as a potential strategy for the treatment of monogenic diseases has certain advantages over traditional gene therapy approaches. Unlike DNA, mRNA does not need to enter the nucleus, which allows for more efficient protein production and does not carry the risk of random integration or mutagenesis.<sup>21,22</sup>

We have examined the efficacy of mRNA therapy in a liver-specific G6PC-deficient mouse model (*L-G6PC<sup>-/-</sup>*), using G6PC mRNA expressing human G6Pase. The *L-G6PC<sup>-/-</sup>* mouse model closely resembles the human hepatic pathology of GSD1a and translates well to human disease.<sup>3,8</sup> Systemic administration of lipid nanoparticle (LNP)-encapsulated G6PC mRNA delivered mRNA to liver hepatocytes, where the mRNA is released into the cytosol and expresses a functional G6Pase enzyme. To improve upon the intracellular duration of the G6Pase protein, several protein-engineered variants (variant 1 [V1] and variant 2 [V2]) were designed based on algorithms for increased thermostability. Our results show that the G6PC mRNA can be successfully delivered to the liver, expressing active G6Pase protein that corrects hypoglycemia and significantly reduces the hepatic abnormalities associated with GSD1a.

Received 13 September 2017; accepted 9 January 2018;  
<https://doi.org/10.1016/j.ymthe.2018.01.006>

**Correspondence:** Romesh R. Subramanian, Discovery Research, Alexion Pharmaceuticals, Inc., 75 Sidney Street, Cambridge, MA 02139, USA.

**E-mail:** [romesh.r.subramanian@gmail.com](mailto:romesh.r.subramanian@gmail.com)



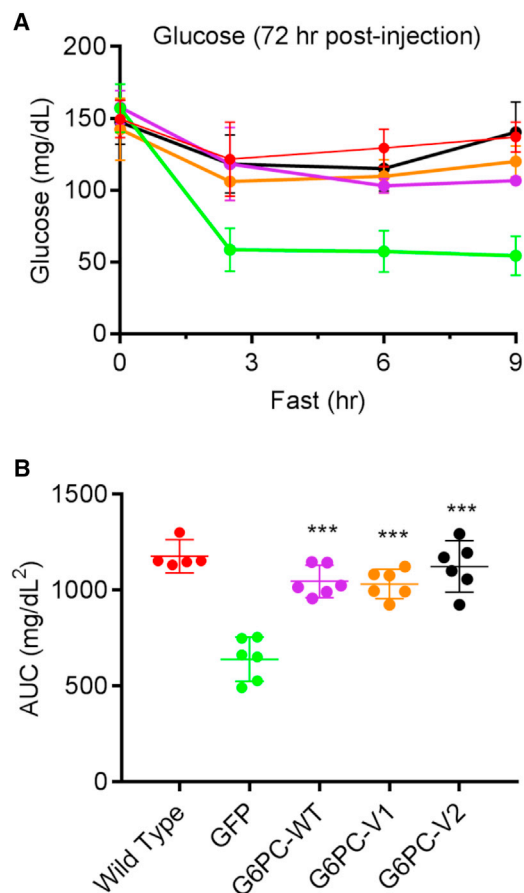


**Figure 1. Effect of mRNA Therapy after 72 hr on Fasting Glycemia**

(A) Fasting blood glucose levels were monitored for 9 hr in GFP mRNA-treated WT mice (red circles), GFP mRNA-treated *L.G6PC*<sup>-/-</sup> mice (green circles), G6PC-WT-treated *L.G6PC*<sup>-/-</sup> mice (purple circles), G6PC-V1-treated *L.G6PC*<sup>-/-</sup> mice (orange circles), and G6PC-V2-treated *L.G6PC*<sup>-/-</sup> mice (black circles). (B) Areas under the curve (AUCs) were calculated from each fasting glucose curve, and individual treatment groups (n = 5 or 6) are shown, with bars representing the mean ± 95% confidence interval (CI). The groups were compared by one-way ANOVA followed by Dunnett's comparison test. Values significantly different from GFP-treated *L.G6PC*<sup>-/-</sup> mice (\*\*\*) are indicated.

## RESULTS

### Correction of Fasting Blood Glucose after mRNA Therapy in *L-G6PC*<sup>-/-</sup> Mice

To examine the efficacy of mRNA therapy in hepatic G6PC null mice, human G6PC mRNAs encoding wild-type G6Pase and several protein-engineered sequences were formulated into LNPs and evaluated in inducible liver *L-G6PC*<sup>-/-</sup> mice. *L-G6PC*<sup>-/-</sup> mice have an absence of liver G6Pase activity and are therefore unable to induce gluconeogenesis and glycogenolysis in the liver, which in the absence of an alternative source of glucose, leads to severe hypoglycemia during the fasting state. However, the mice are able to maintain normoglycemia during a non-fasting state due to a compensatory increase in G6Pase in the kidney and small intestine. Therefore, efficacy of G6PC mRNAs was evaluated in *L-G6PC*<sup>-/-</sup> mice subjected to

fasting-induced hypoglycemia. Mice were injected with 1 mg/kg mRNAs intravenously, and fasting was initiated 72 hr after injection. In previous studies, *L-G6PC*<sup>-/-</sup> mice became hypoglycemic after 6 hr of fasting, with blood glucose levels dropping to 40–50 mg/dL, compared to wild-type mice, whose levels range from 150 to 160 mg/dL.<sup>23</sup> To allow for a more detailed assessment across all treatment groups, blood glucose levels were measured at 2.5, 6, and 9 hr after the start of fasting, and the areas under the curve (AUCs) were calculated (Figures 1A and 1B). The GFP mRNA-treated control group showed a fasting blood glucose curve similar to that reported previously in *L-G6PC*<sup>-/-</sup> mice, with an area under the curve found to be approximately 50% of that found with wild-type mice.<sup>23</sup> However, treatment with human G6PC-wild-type (WT), G6PC-V1, and G6PC-V2 mRNAs achieved near-normal blood glucose levels. These results demonstrate that mRNA treatment can restore normoglycemia in fasting *L-G6PC*<sup>-/-</sup> mice beyond 72 hr.

### Correction of Hepatic Biomarkers and Histological Abnormalities after mRNA Therapy in *L-G6PC*<sup>-/-</sup> Mice

*L-G6PC*<sup>-/-</sup> mice exhibit the hallmark liver pathologies associated with GSD1a patients, including hepatomegaly and steatosis that is caused by increased hepatocellular pools of G6P, glycogen, and triglycerides.<sup>8,23</sup> The effect of mRNA treatment on liver size and hepatic biomarker content of G6P, glycogen, and triglycerides was examined 96 hr after injection (post-24-hr fast) (Figure 2). The livers of the GFP mRNA-treated control groups accounted for 9.5% of total body mass compared to the livers of the WT animals, which accounted for 3.8% of total body mass (Figure 2A). Treatment with human G6PC-WT, G6PC-V1, and G6PC-V2 mRNAs reduced the liver/body weight (BW) ratio to 6.7%, 5.8%, and 5.6%, respectively. This reduction in liver/BW ratio was associated with significant reductions in liver G6P, glycogen, and triglycerides (Figures 2B–2D). Reductions in liver G6P with human G6PC-WT, G6PC-V1, and G6PC-V2 mRNAs were 63%, 33%, and 34%, respectively (Figure 2B), while liver glycogen was reduced 50%, 23%, and 29%, respectively (Figure 2C). In addition, liver triglycerides were reduced to WT levels in all treatment groups (Figure 2D).

Histological analysis of liver biopsy samples from fasting WT and liver-specific G6PC null mouse model (*L.G6PC*<sup>-/-</sup>) mice is shown in Figure 3. Compared to WT mice, the hepatocytes in the *L.G6PC*<sup>-/-</sup> mice are devoid of G6PC staining and show morphological abnormalities (Figures 3Aa and 3Ab). However, treatment with human G6PC-WT, G6PC-V1, and G6PC-V2 mRNAs resulted in a dramatic reduction in hepatocyte vacuolization and normalization in morphology 24 hr post-treatment (data not shown), which was still observed at 96 hr (Figures 3Ac–3Ae). In addition, G6PC mRNA was localized to hepatocytes 24 hr post-treatment (Figure 3B), although G6PC protein was still detected in some hepatocytes at 96 hr post-treatment (Figures 3Ac–3Ae). G6PC mRNA was undetectable beyond 24 hr by both histological analysis (*in situ* hybridization [ISH]) and qPCR (data not shown).

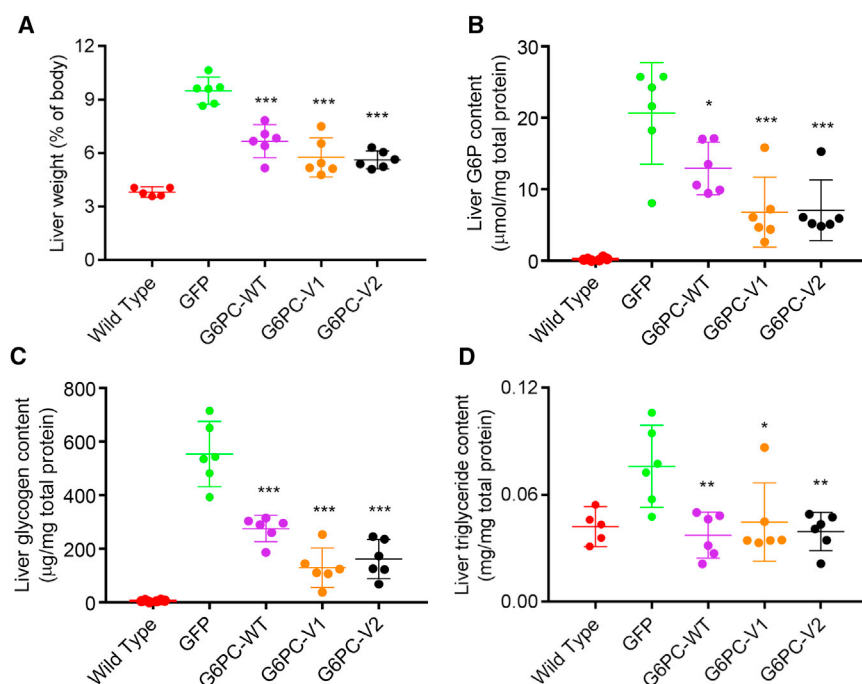


**Figure 2. Effect of mRNA Therapy after 96 hr on Hepatic Biomarkers**

(A) Liver weight as percentage of total body weight, (B) hepatic G6P content, (C) hepatic glycogen content, and (D) hepatic triglyceride content in GFP mRNA-treated WT mice (red circles), GFP mRNA-treated *L.G6PC*<sup>-/-</sup> mice (green circles), G6PC-WT-treated *L.G6PC*<sup>-/-</sup> mice (purple circles), G6PC-V1-treated *L.G6PC*<sup>-/-</sup> mice (orange circles), and G6PC-V2-treated *L.G6PC*<sup>-/-</sup> mice (black circles). Data were obtained from mice fasted for 24 hr, and individual treatment groups (n = 5 or 6) are shown, with bars representing the mean  $\pm$  95% CI. The groups were compared by one-way ANOVA followed by Dunnett's comparison test. Values significantly different from GFP-treated *L.G6PC*<sup>-/-</sup> mice (\*p < 0.05, \*\*p < 0.005, and \*\*\*p < 0.0005) are indicated.

### Protein-Engineered Human G6Pase Sequence Can Sustain Efficacy for 12 Days

We have designed a proprietary protein engineering strategy for increasing expression and intracellular half-life (J.D.F, K.H. Asrani, C.I., J.S. deBear, M.R. Stahley, A. Shah, M.A. Lasaro, C.J. Cheng, R.R.S., unpublished data). Initial screening of variants was performed in primary human hepatocytes to identify candidates based on duration of G6Pase expression and/or activity over time (data not shown). To confirm the findings of the initial screening, human G6PC-WT, G6PC-V1, and G6PC-V2 mRNAs were expressed in primary human hepatocytes and G6Pase protein expression was monitored over time by western blot analysis (Figure 4). Visual analysis of the protein bands over time demonstrates that both engineered G6Pase variants had a longer duration of protein expression than the parent WT sequence *in vitro*, potentially sustaining expression to 14 days.

To determine whether the *in vitro* results translate *in vivo*, an animal study similar to the one described earlier was performed and the effect on hypoglycemia was evaluated at extended time points to differentiate among the efficacies of the different G6PC sequences. Fasting was initiated 6 and 11 days after a single dose of mRNA, and the ability to improve hypoglycemia was evaluated for each of the human G6PC mRNA constructs against the control GFP group (Figure 5). Treatment with human G6PC-WT mRNA failed to improve fasting blood glucose levels at 6 days post-dose (Figures 5A and 5C). However, both the human G6PC-V1 and the human G6PC-V2 mRNA-treated groups showed significant improvements in fasting blood glucose levels on day 6 post-dose (p < 0.05 and p < 0.0005, respectively). Similarly, livers collected from G6PC-V1

and G6PC-V2 mRNA-treated groups 7 days (24-hr fast) after injection showed significant reductions in the liver/BW ratio (p < 0.05 and p < 0.0005, respectively) (Figure 6A). Beyond 11 days post-dose, only the G6PC-V2 mRNA-treated *L.G6PC*<sup>-/-</sup> mice continued to show significant improvements in fasting blood glucose levels (p < 0.0005) (Figures 5B and 5D). This correlated with findings that only the G6PC-V2 mRNA-treated group maintained significant reductions in the liver/BW ratio (p < 0.0005) to 12 days (Figure 6B). Furthermore, enzyme activity levels were found to be approximately 2%–4% of the levels for WT animals (data not shown), suggesting that activity could be therapeutically relevant.<sup>10</sup>

### DISCUSSION

In this report, we demonstrate that a single administration of LNP-encapsulated G6PC mRNA expressing human G6Pase was successful in correcting G6Pase deficiency in *L-G6PC*<sup>-/-</sup> mice. The treated mice achieved normal fasting blood glucose levels and partial alleviation of hepatomegaly, with associated reductions in hepatic triglycerides and glycogen. To overcome the limitations of transient correction associated with mRNA-based therapy, we protein-engineered variants of human glucose-6-phosphatase (huG6Pase) for increased intracellular expression. Efficacy of V2 was still detectable at 12 days post-dose with 2%–4% of WT G6Pase activity, along with corrected hypoglycemia and reduced hepatomegaly. A study assessing the efficacy of recombinant adeno-associated virus (rAAV)-G6PC-mediated therapy in total *G6PC*<sup>-/-</sup> mice reported that a minimum of 2% of WT G6Pase activity is required to maintain glucose homeostasis and prevent liver HCA formation.<sup>15</sup> Our data suggest that protein-engineered variants of G6Pase can make mRNA therapy a viable option for the treatment of human GSD1a.

In the absence of a dietary source for blood glucose, GSD1a is lethal, and most patients cannot survive infancy. The implementation of strict dietary guidelines has dramatically improved the life

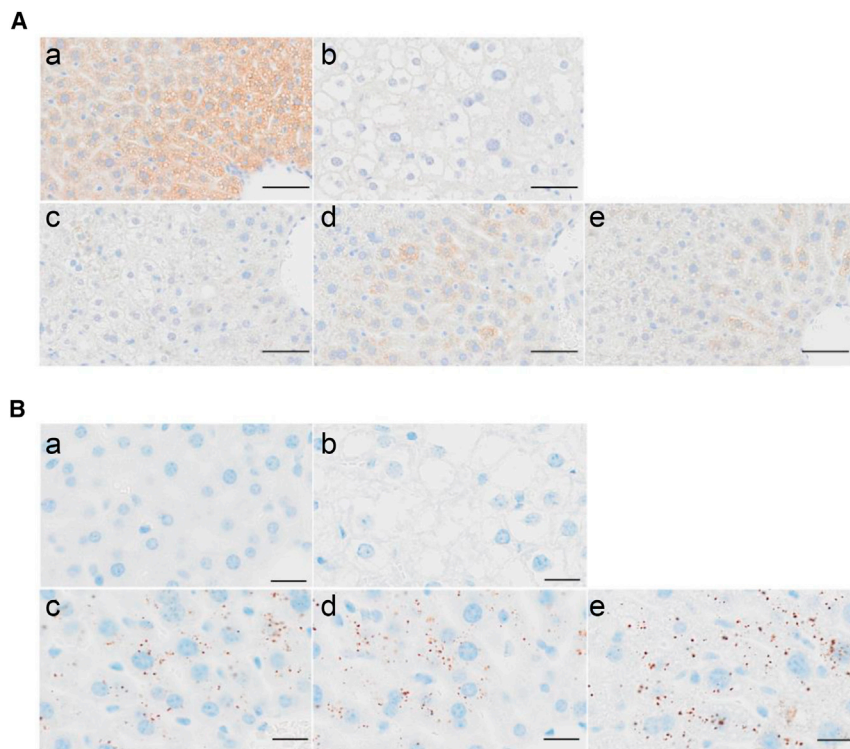


**Figure 3. Histological Analysis of the Liver after mRNA Therapy**

(A) Immunohistochemistry (IHC) of G6PC (brown staining) in the liver of (a) WT mice and (b) untreated *L.G6PC*<sup>-/-</sup> mice. Note vacuolated hepatocytes in the *L.G6PC*<sup>-/-</sup> sample. Immunohistochemistry of G6PC in the liver of *L.G6PC*<sup>-/-</sup> mice treated with (c) G6PC-WT, (d) G6PC-V1, and (e) G6PC-V2 mRNA at 96 hr post-treatment. Note the reduction of hepatocyte vacuolization and return to more WT-like hepatocyte morphology in the cells closest to the vein. (B) Distribution of human G6PC mRNA (brown dots) at 24 hr post-treatment in (a) WT mice, (b) GFP mRNA-treated *L.G6PC*<sup>-/-</sup> mice, (c) G6PC-WT-treated *L.G6PC*<sup>-/-</sup> mice, (d) G6PC-V1-treated *L.G6PC*<sup>-/-</sup> mice, and (e) G6PC-V2-treated *L.G6PC*<sup>-/-</sup> mice.

expectancy of GSD1a patients, but long-term hepatic and renal complications arise with aging. Liver transplantation can successfully normalize the metabolic sequelae and correct fasting tolerance in GSD1a patients, highlighting the potential of liver-based therapies.<sup>24</sup>

Several animal models have been generated to study the pathologies of GSD1a, including a mouse model of total G6PC deficiency.<sup>25</sup> However, these mice display a phenotype more severe than that of GSD1a patients, because neonatal mortality is high, with only a 15% survival rate through weaning.<sup>9</sup> More recently, a *L.G6PC*<sup>-/-</sup> was developed.<sup>23</sup> These mice have a normal life expectancy but manifest the hepatic pathology closest to that of GSD1a patients, including the late onset of HCAs and HCCs.

Gene therapy has been successfully used to correct the pathologies associated with GSD1a in both mouse and dog models. However, clinical feasibility remains elusive, likely due to the inherent risks associated with gene therapy. mRNA offers several advantages as a therapeutic alternative to gene therapy, including efficient protein expression without the need to first enter the nucleus and absence of random integration risks. Unlike the reported long-term expression associated with gene therapy, protein expression via mRNA-mediated delivery is transient and, like protein-based therapeutics, requires long-term chronic dosing. Efficacy that is sustainable should rely on the translational efficiency and intracellular stability of the mRNA, as well as the intracellular half-life of the translated

protein. Protein engineering to improve the intracellular stability of a protein is a new concept that complements mRNA-based therapeutics. It is possible that the improvements seen with the current G6PC variants would be more pronounced in humans, because murine G6Pase was not tested in the current study. Improved screening strategies help identify even longer-lasting G6Pase variants with improved efficacy beyond 2 weeks.

This is the first study showing mRNA therapy as a viable option for the treatment of G6Pase deficiency and warrants further multi-dose studies in larger animals, such as the GSD1a-deficient dog model.

## MATERIALS AND METHODS

### Generation of Liver-Specific G6PC Null Mice

The liver-specific G6Pase- $\alpha$  mice were generated by a specific deletion of G6PC exon 3 in the liver using a CRE-lox strategy in mice, as described.<sup>23</sup> Male adult B6.G6PC<sup>lox/lox</sup>.SA<sup>creERT2/w</sup> and control C57BL/6J mice (6–8 week old) were injected intraperitoneally once daily with 100  $\mu$ L of tamoxifen (10 mg/mL, Sigma) on five consecutive days to obtain *L.G6PC*<sup>-/-</sup> and *L.G6PC*<sup>+/+</sup> mice. Five to seven weeks following tamoxifen induction, mice were enrolled in metabolic studies. All mice were maintained in a controlled environment (22°C) on a 12-hr light/12-hr dark cycle. Mice were provided with *ad libitum* access to water and standard rodent chow diet, with the exception of fasted mice that were only provided access to water. All animal studies were conducted at the animal facility of Lyon 1 University and were performed in accordance with the principles and guidelines established by the European Convention for the Protection of Laboratory Animals. All protocols were approved by the animal care committee of the university.

### Metabolic Studies

Control GFP or human G6PC-WT, G6PC-V1, or G6PC-V2 mRNAs were LNP encapsulated and administered to mice by tail vein injection at 1 mg/kg body weight. Fasted mice were transferred to cages

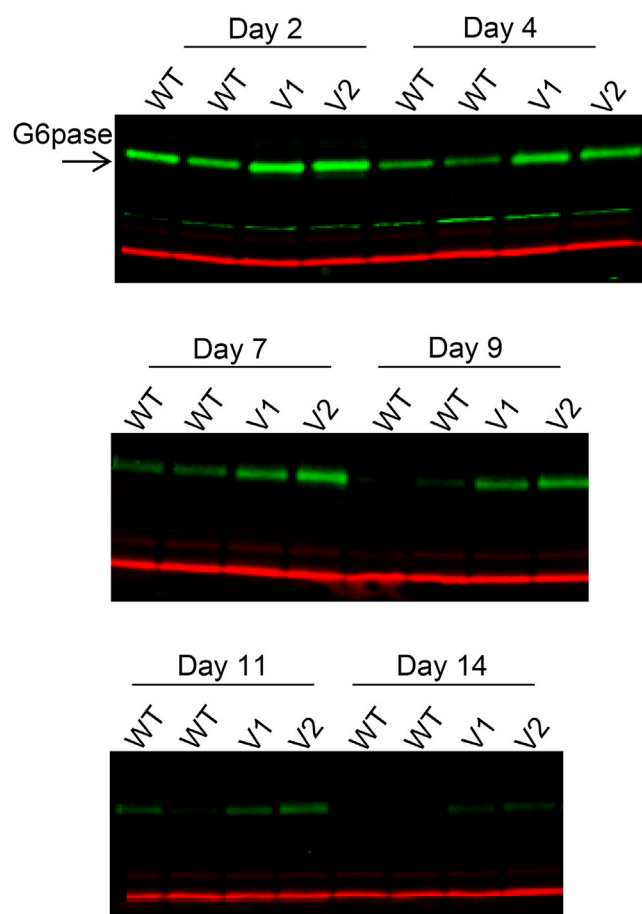


**Figure 4. Western Blot Analysis of G6Pase Expression over Time in Human Primary Hepatocytes Transfected with WT or Protein-Engineered mRNAs**  
Cells transfected with human G6PC-WT (WT), G6PC-V1 (V1), and G6PC-V2 (V2) mRNAs were lysed at the indicated days post-transfection and analyzed via western blot using a rabbit anti-human G6Pase polyclonal Ab.

with new bedding. Blood glucose was monitored by tail bleed at the indicated time points using a glucometer. Terminal blood was collected at the 24-hr fasting time point by submandibular bleed and processed for serum or plasma. Mice were then euthanized, and a portion of the liver was stored in RNAlater (Invitrogen) for mRNA analysis, while the remaining liver was immediately snap-frozen for liver metabolite analysis.

#### Liver Glucose-6-Phosphate, Glycogen, and Triglyceride Measurements

Snap-frozen liver samples were homogenized using the Precellys lysing kit in PBS (Gibco) containing protease inhibitors (Thermo Fisher Scientific) at a volume of 10  $\mu$ L/mg tissue. All samples were centrifuged at 500  $\times$  g for 3 min at 4°C before protein quantification using the detergent compatible (DC) protein assay (Bio-Rad). Glycogen was measured in 100- to 400-fold diluted liver homogenates using a fluorescent plate-based assay (Cayman Chemical) according

to the manufacturer's protocol, with one modification of mixing at 250 rpm during the 37°C incubation steps. Liver G6P content was measured in 400- to 800-fold diluted liver homogenates using a fluorescent plate-based assay (Abcam) as described in the manufacturer's protocol. Livers were assayed for the presence of triglycerides using the Triglyceride Colorimetric Assay Kit according to the manufacturer's instructions (Cayman Chemical), with the exception of using Precellys lysing kits (Bertin Instruments) to perform the homogenization step. Briefly, 25–50 mg liver samples were thawed on ice in Precellys lysing kit tubes in 10  $\mu$ L of ice-cold nonyphenoxypolyethoxyethanol (NP40) Substitute Assay Reagent with protease inhibitors (Thermo Fisher Scientific) and processed using Precellys 24 at 4°C and 2,500 rpm for 2 rounds of 20 s each, followed by centrifugation at 10,000  $\times$  g for 10 min at 4°C.

The glycogen, G6P, and triglyceride assay plates were read in a SpectraMax M3 plate reader with non-linear regression (4 parameters logistic [4PL]) standard curve fit, and analyte levels were interpolated from the curve using SoftMaxPro software v.6.4.1. Total protein concentration was used to normalize each sample measurement for all analytes.

#### Immunohistochemistry and ISH Procedures

Formalin-fixed, paraffin-embedded (FFPE) tissues were prepared at 5  $\mu$ m thickness on glass slides. Immunohistochemistry was performed by the Leica BOND RX platform using rabbit anti-G6PC polyclonal antibody (PAb) (Atlas Antibodies) primary antibody followed by diaminobenzidine (DAB) chromogenic detection. For negative control, rabbit immunoglobulin G (IgG) was used at the same concentration. Slides were serially dehydrated in a graded ethanol series, cleared in xylene, and mounted using Cytoseal. Slides were imaged using the VS120 system at 40 $\times$  magnification (Olympus).

For mRNA visualization, ISH was used. Custom RNA ISH probes (Advanced Cell Diagnostics) were designed to detect the modified G6PC mRNA. RNAscope assays were performed using the RNAscope 2.0 FFPE Brown Reagent kit, and the Leica BOND RX platform was used for the automated assay. FFPE tissues were prepared at 5  $\mu$ m thickness on glass slides and put on the Leica BOND RX. The single-plex RNAscope assay was run according to the manufacturer's protocol: sections were baked and deparaffinized on the instrument, followed by target retrieval (15 min at 95°C for tissues using Leica Epitope Retrieval Buffer 2) and protease treatment (15 min at 40°C). Probes were then hybridized for 2 hr at 42°C followed by RNAscope amplification and DAB chromogenic detection. To ensure RNA integrity and assay procedure, additional sections were hybridized with a probe for peptidyl prolyl isomerase B (PPIB) mRNA, an endogenous housekeeping protein. To account for non-specific staining, a probe against bacterial protein dihydrodipicolinate reductase (dapB) was used as a negative control. Slides were serially dehydrated in a graded ethanol series, cleared in xylene, and mounted using Cytoseal. Slides were imaged using the VS120 system at 40 $\times$  magnification (Olympus).

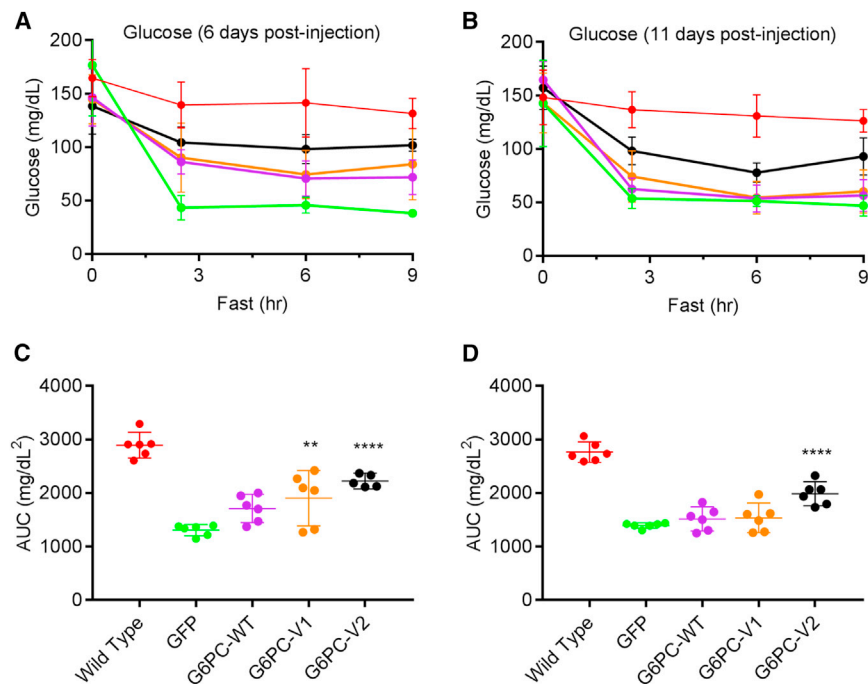


**Figure 5. Effect of mRNA Therapy on Fasting Glycemia 6 and 11 Days Post-Treatment**

Plot of fasting blood glucose levels to 9 hr following (A) 6 days and (B) 11 days of mRNA dosing. GFP mRNA-treated WT mice (red circles), GFP mRNA-treated *L.G6PC*<sup>-/-</sup> mice (green circles), G6PC-WT-treated *L.G6PC*<sup>-/-</sup> mice (purple circles), G6PC-V1-treated *L.G6PC*<sup>-/-</sup> mice (orange circles), and G6PC-V2-treated *L.G6PC*<sup>-/-</sup> mice (black circles). AUCs were calculated from the plots of (C) 6 days and (D) 11 days, and individual treatment groups (n = 5 or 6) are shown, with bars representing the mean ± 95% CI. The groups were compared by one-way ANOVA followed by Dunnett's comparison test. Values significantly different from GFP-treated *L.G6PC*<sup>-/-</sup> mice (\*\*p < 0.005 and \*\*\*\*p < 0.0001) are indicated.

### G6Pase Enzyme Activity

For preparation of microsomes, 0.4 g of snap-frozen liver samples were each homogenized by a Polytron in 4 mL of 0.9% sodium chloride solution. To this was added 6 mL of microsome separation (MS) buffer (4 mM sodium chloride with 2% glycerol), and the sample was centrifuged at 12,000 × g for 20 min at 4°C. The pellets were discarded, and the supernatants were then centrifuged at 105,000 × g for 1 hr at 4°C. The pellets (microsomes) were suspended in 0.4 mL of MS buffer, and protein was quantitatively determined using the bicinchoninic acid (BCA) assay (Thermo Fisher Scientific). G6Pase activity was measured with a modified version of the Taussky-Shorr method.<sup>26</sup> Briefly, 20 μg of microsomes were added to 50 mM G6P in 100 mM Bis/Tris buffer (pH 6.5) (total volume of 200 μL) and incubated for 30 min at 37°C.

### In Vitro Screening of G6PC mRNAs

Primary human hepatocytes were procured from the *In Vitro* ADMET Laboratory (IVAL). Cultured cells plated in 24-well collagen-coated plates were received on the day of transfection, and the medium was changed to hepatocyte induction medium (HIM) supplemented with the HIM supplement kit (IVAL) for cells to equilibrate for 2 hr at 37°C with 5% CO<sub>2</sub> before transfection. To ensure that primary hepatocytes were healthy during the extended period of study, a 14-day time course was performed. Media were changed every 2 days to maintain the health and viability of cells, and observations were made by microscopy.

Primary human hepatocytes were transfected with 2.5 μg of each mRNA and 6 μL of mRNA-In lipid transfection reagent (MTI-

GlobalStem). Each mRNA was diluted to 2.5 μg in OptiMEM (Gibco), a similarly appropriate volume of mRNA-In was diluted in OptiMEM per well, and the protocol was followed according to the manufacturer's recommendation. Diluted mRNA was mixed with diluted lipid and allowed to incubate for 15 min at room temperature before it was added to cells. After addition of mRNA-lipid mix to hepatocytes, cells were returned to the incubator at 37°C with 5% CO<sub>2</sub>. For collection at appropriate time points, cells were gently washed with PBS (Gibco) twice and lysed in fresh radioimmunoprecipitation assay (RIPA) buffer (Sigma) with 1× protease inhibitors (Sigma). Primary human hepatocytes were collected at days 1, 2, 5, 7, 9, and 12 post-transfection.

The cell lysates were collected in 0.5 mL tubes (Eppendorf) and clarified by centrifugation at 18,000 × g at 4°C to remove cell debris. After centrifugation, clear supernatant was carefully transferred to a separate labeled tube and placed on ice. Special care was taken to keep lysates on ice to ensure stability of target G6PC protein. Total protein concentration was determined with a BCA assay kit (Thermo Fisher Scientific) in duplicate, in a 96-well format according to the manufacturer's protocol.

Cell lysates were prepared for western blots on the same day as the BCA assay. Fluorescence western blots were obtained with rabbit anti-G6PC PAb (Atlas Antibodies) primary antibody and mouse anti-COX-IV monoclonal antibody (mAb) as housekeeper (Cell Signaling Technology). 25 μg of total protein diluted in water was denatured in 2× Laemmle buffer (Santa Cruz, sc-286962) and heated at 70°C for 10 min. After denaturation, samples were loaded on Bis-Tris 4%–12% gels (Thermo Fisher Scientific). Samples were run on a mini-gel tank for 50 min at 160 V, with a constant current of 200 A. After running gels, proteins were transferred to a nitrocellulose membrane using iBlot transfer stacks (Thermo Fisher Scientific). The membranes were blocked in Odyssey blocking buffer

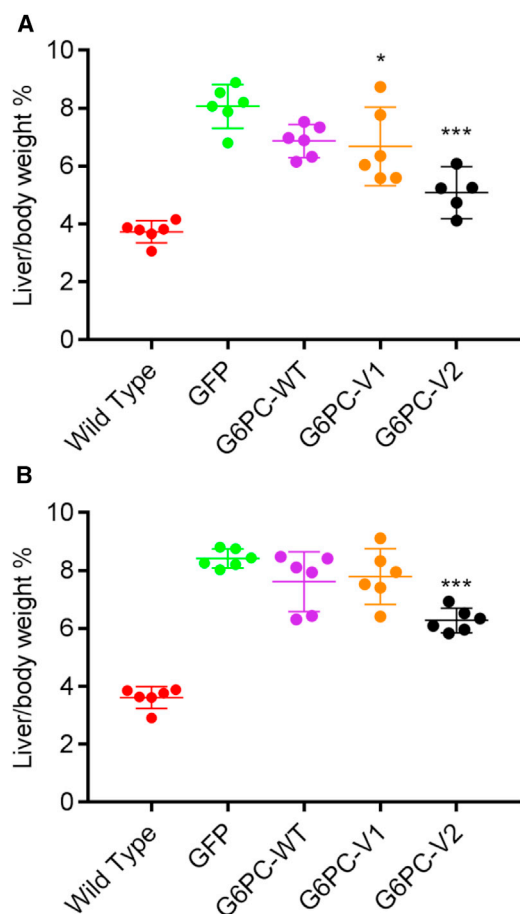


**Figure 6. Effect of mRNA Therapy on Liver Weight at 7 and 12 Days**

Liver weight as a percentage of total body weight after (A) 7 days or (B) 12 days post-dose. GFP mRNA-treated WT mice (red circles), GFP mRNA-treated *L.G6PC*<sup>-/-</sup> mice (green circles), G6PC-WT-treated *L.G6PC*<sup>-/-</sup> mice (purple circles), G6PC-V1-treated *L.G6PC*<sup>-/-</sup> mice (orange circles), and G6PC-V2-treated *L.G6PC*<sup>-/-</sup> mice (black circles). Data were obtained from mice fasted for 24 hr, and individual treatment groups (n = 5 or 6) are shown, with bars representing the mean  $\pm$  95% CI. The groups were compared by one-way ANOVA followed by Dunnett's comparison test. Values significantly different from GFP-treated *L.G6PC*<sup>-/-</sup> mice (\*p < 0.05, \*\*p < 0.005, and \*\*\*p < 0.0005) are indicated.

(LI-COR Biosciences) for 1 hr and incubated overnight at 4°C in a cocktail of a 1:750 concentration of primary antibody and recommended dilution of housekeeper diluted in Odyssey buffer with 0.1% Tween 20 (Sigma). The next day, membranes were washed on SNAP-ID 2.0 (EMD Millipore) with 1× Tris-buffered saline (TBS) (Thermo Fisher Scientific) + 1% Tween 20 four times and incubated for 10 min with a cocktail of goat anti-rabbit (LI-COR Biosciences) and goat anti-mouse (LI-COR Biosciences) secondary antibodies diluted in antibody buffer, and the SNAP-ID 2.0 protocol was followed according to the instructions provided by the manufacturer. Membranes were washed again four times with 1× TBS on SNAP-ID 2.0 and removed to be imaged on an Odyssey CLx Imaging System (LI-COR Biosciences).

### Statistical Analyses

Statistical analysis was performed using one-way ANOVA followed by Dunnett's comparison test with GraphPad Prism v.7.0 (GraphPad, San Diego, CA). Area under the curve (AUC) calculations were determined using the AUC analysis tool in GraphPad Prism. Statistical significance was defined as \*p < 0.05, \*\*p < 0.005, and \*\*\*p < 0.0005, or as otherwise indicated.

### AUTHOR CONTRIBUTIONS

D.S.R., T.K., and R.R.S. designed experiments; D.S.R., T.K., F.R., L.S.J., K.H.A., C.L., and J.D.F. conducted experiments; D.S.R. and R.R.S. wrote the paper.

### CONFLICTS OF INTEREST

All authors are employees and shareholders of Alexion Pharmaceuticals, a company that develops therapies for rare and ultra-rare diseases.

### ACKNOWLEDGMENTS

The authors acknowledge Linda Crew for biomarker support. Funding for open access charge was provided by Alexion Pharmaceuticals.

### REFERENCES

- Shelly, L.L., Lei, K.J., Pan, C.J., Sakata, S.F., Ruppert, S., Schutz, G., and Chou, J.Y. (1993). Isolation of the gene for murine glucose-6-phosphatase, the enzyme deficient in glycogen storage disease type 1A. *J. Biol. Chem.* 268, 21482–21485.
- Froissart, R., Piraud, M., Boudjemline, A.M., Vianey-Saban, C., Petit, F., Hubert-Buron, A., Eberschweiler, P.T., Gajdos, V., and Labrune, P. (2011). Glucose-6-phosphatase deficiency. *Orphanet J. Rare Dis.* 6, 27.
- Rajas, F., Clar, J., Gautier-Stein, A., and Mithieux, G. (2015). Lessons from new mouse models of glycogen storage disease type 1a in relation to the time course and organ specificity of the disease. *J. Inher. Metab. Dis.* 38, 521–527.
- Chou, J.Y., Jun, H.S., and Mansfield, B.C. (2010). Glycogen storage disease type I and G6Pase- $\beta$  deficiency: etiology and therapy. *Nat. Rev. Endocrinol.* 6, 676–688.
- Bruni, N., Rajas, F., Montano, S., Chevalier-Porst, F., Maire, I., and Mithieux, G. (1999). Enzymatic characterization of four new mutations in the glucose-6 phosphatase (G6PC) gene which cause glycogen storage disease type 1a. *Ann. Hum. Genet.* 63, 141–146.
- Chou, J.Y., Matern, D., Mansfield, B.C., and Chen, Y.T. (2002). Type I glycogen storage diseases: disorders of the glucose-6-phosphatase complex. *Curr. Mol. Med.* 2, 121–143.
- Rake, J.P., Visser, G., Labrune, P., Leonard, J.V., Ullrich, K., and Smit, G.P.; European Study on Glycogen Storage Disease Type I (ESGSD I) (2002). Guidelines for management of glycogen storage disease type I—European Study on Glycogen Storage Disease Type I (ESGSD I). *Eur. J. Pediatr.* 161 (Suppl 1), S112–S119.
- Clar, J., Mutel, E., Gri, B., Creneguy, A., Stefanutti, A., Gaillard, S., Ferry, N., Beuf, O., Mithieux, G., Nguyen, T.H., and Rajas, F. (2015). Hepatic lentiviral gene transfer prevents the long-term onset of hepatic tumours of glycogen storage disease type 1a in mice. *Hum. Mol. Genet.* 24, 2287–2296.
- Koeberl, D.D., Sun, B., Bird, A., Chen, Y.T., Oka, K., and Chan, L. (2007). Efficacy of helper-dependent adenovirus vector-mediated gene therapy in murine glycogen storage disease type 1a. *Mol. Ther.* 15, 1253–1258.
- Lee, Y.M., Kim, G.Y., Pan, C.J., Mansfield, B.C., and Chou, J.Y. (2015). Minimal hepatic glucose-6-phosphatase- $\alpha$  activity required to sustain survival and prevent hepatocellular adenoma formation in murine glycogen storage disease type 1a. *Mol. Genet. Metab. Rep.* 3, 28–32.
- Wang, D.Q., Fiske, L.M., Carreras, C.T., and Weinstein, D.A. (2011). Natural history of hepatocellular adenoma formation in glycogen storage disease type I. *J. Pediatr.* 159, 442–446.



12. Franco, L.M., Krishnamurthy, V., Bali, D., Weinstein, D.A., Arn, P., Clary, B., Boney, A., Sullivan, J., Frush, D.P., Chen, Y.T., and Kishnani, P.S. (2005). Hepatocellular carcinoma in glycogen storage disease type Ia: a case series. *J. Inher. Metab. Dis.* 28, 153–162.
13. Calderaro, J., Labrune, P., Morcrette, G., Rebouissou, S., Franco, D., Prévot, S., Quaglia, A., Bedossa, P., Libbrecht, L., Terracciano, L., et al. (2013). Molecular characterization of hepatocellular adenomas developed in patients with glycogen storage disease type I. *J. Hepatol.* 58, 350–357.
14. Zingone, A., Hiraiwa, H., Pan, C.J., Lin, B., Chen, H., Ward, J.M., and Chou, J.Y. (2000). Correction of glycogen storage disease type Ia in a mouse model by gene therapy. *J. Biol. Chem.* 275, 828–832.
15. Kim, G.Y., Lee, Y.M., Kwon, J.H., Cho, J.H., Pan, C.J., Starost, M.F., Mansfield, B.C., and Chou, J.Y. (2017). Glycogen storage disease type Ia mice with less than 2% of normal hepatic glucose-6-phosphatase- $\alpha$  activity restored are at risk of developing hepatic tumors. *Mol. Genet. Metab.* 120, 229–234.
16. Weinstein, D.A., Correia, C.E., Conlon, T., Specht, A., Versteegen, J., Onclin-Versteegen, K., Campbell-Thompson, M., Dhaliwal, G., Mirian, L., Cossette, H., et al. (2010). Adeno-associated virus-mediated correction of a canine model of glycogen storage disease type Ia. *Hum. Gene Ther.* 21, 903–910.
17. Crane, B., Luo, X., Demaster, A., Williams, K.D., Kozink, D.M., Zhang, P., Brown, T.T., Pinto, C.R., Oka, K., Sun, F., et al. (2012). Rescue administration of a helper-dependent adenovirus vector with long-term efficacy in dogs with glycogen storage disease type Ia. *Gene Ther.* 19, 443–452.
18. Demaster, A., Luo, X., Curtis, S., Williams, K.D., Landau, D.J., Drake, E.J., Kozink, D.M., Bird, A., Crane, B., Sun, F., et al. (2012). Long-term efficacy following readministration of an adeno-associated virus vector in dogs with glycogen storage disease type Ia. *Hum. Gene Ther.* 23, 407–418.
19. Brooks, E.D., Little, D., Arumugam, R., Sun, B., Curtis, S., Demaster, A., Maranzano, M., Jackson, M.W., Kishnani, P., Freemark, M.S., and Koerber, D.D. (2013). Pathogenesis of growth failure and partial reversal with gene therapy in murine and canine Glycogen Storage Disease type Ia. *Mol. Genet. Metab.* 109, 161–170.
20. Hareendran, S., Balakrishnan, B., Sen, D., Kumar, S., Srivastava, A., and Jayandharan, G.R. (2013). Adeno-associated virus (AAV) vectors in gene therapy: immune challenges and strategies to circumvent them. *Rev. Med. Virol.* 23, 399–413.
21. Zangì, L., Lui, K.O., von Gise, A., Ma, Q., Ebina, W., Ptaszek, L.M., Später, D., Xu, H., Tabebordbar, M., Gorbатов, R., et al. (2013). Modified mRNA directs the fate of heart progenitor cells and induces vascular regeneration after myocardial infarction. *Nat. Biotechnol.* 31, 898–907.
22. Sun, L., Xiong, Y., Bashan, A., Zimmerman, E., Shulman Daube, S., Peleg, Y., Albeck, S., Unger, T., Yonath, H., Krupkin, M., et al. (2015). A recombinant collagen-mRNA platform for controllable protein synthesis. *ChemBioChem* 16, 1415–1419.
23. Mutel, E., Abdul-Wahed, A., Ramamonjisoa, N., Stefanutti, A., Houberton, I., Cavassila, S., Pilleul, F., Beuf, O., Gautier-Stein, A., Penhoat, A., et al. (2011). Targeted deletion of liver glucose-6 phosphatase mimics glycogen storage disease type Ia including development of multiple adenomas. *J. Hepatol.* 54, 529–537.
24. Boers, S.J., Visser, G., Smit, P.G., and Fuchs, S.A. (2014). Liver transplantation in glycogen storage disease type I. *Orphanet J. Rare Dis.* 9, 47.
25. Lei, K.J., Chen, H., Pan, C.J., Ward, J.M., Mosinger, B., Jr., Lee, E.J., Westphal, H., Mansfield, B.C., and Chou, J.Y. (1996). Glucose-6-phosphatase dependent substrate transport in the glycogen storage disease type-Ia mouse. *Nat. Genet.* 13, 203–209.
26. Tausky, H.H., and Shorr, E. (1953). A microcolorimetric method for the determination of inorganic phosphorus. *J. Biol. Chem.* 202, 675–685.